

Selective Colorimetric Detection of Mercury(II) Using Silver Nanoparticles-Chitosan

Monica Avissa, Mohammad Alauhdin*

Department of Chemistry, Universitas Negeri Semarang Kampus Sekaran Gunungpati
Semarang 50229, Indonesia

*corresponding author email: m.alauhdin@mail.unnes.ac.id

Received August 20, 2021; Accepted December 30, 2021; Available online March 20, 2022

ABSTRACT. Contamination of the environment by hazardous metal ions has been a major environmental issue for the past several decades. Among several hazardous metals, mercury ion (Hg(II)) is of particular concern as its compounds are extremely toxic. Hence, developing detection methods for traces of Hg(II) ions in aquatic systems is critical for mercury pollution mitigation. One method that can be used to monitor Hg(II) in aquatic systems is colorimetry-based method which is simple, rapid, and low-cost, yet selective and sensitive. The method can be conducted by applying the Localized Surface Plasmon Resonance phenomenon of metal nanoparticles, such as silver nanoparticles. There are non-Hg(II) ions in the aquatic environment that can interfere the measurements. Thus, a selective method is needed to obtain a valid measurement result. Here, we introduced silver nanoparticles-chitosan (AgNPs-Ch) synthesized by chemical reduction as a selective probe of Hg(II) in an aqueous solution. The AgNPs-Ch was synthesized from silver nitrate at 80°C using trisodium citrate and chitosan as reducing agent and stabilizer, respectively. The synthesized nanoparticles were spherical with an average size below 15.0 nm. Moreover, the AgNPs-Ch was selective for Hg(II) with a linearity of 0.9556 in the concentration range of 1 - 5 ppm and was able to detect the ion down to 1.33 ppm.

Keywords: chitosan; colorimetry; mercury(II); silver nanoparticles

INTRODUCTION

Method of measuring transition metal ions is generally carried out through a process that is tedious, expensive, and time consuming. For example, Hg(II) analysis is usually carried out using sophisticated instruments, such as Cold Vapor-Atomic Absorption Spectrophotometry (CV-AAS) (Fernández et al., 2015; Kristian et al., 2015), Inductively Coupled Plasma – Atomic Emission Spectrometry (ICP-AES) (Fernández et al., 2015), Flow Injection Analysis- Atomic Fluorescence Spectroscopy (FIA-AFS) (Zierhut, Leopold, Harwardt, & Schuster, 2010) or Inductively Coupled Plasma – Mass Spectrometry (ICP-MS) (Cheng, Wu, Shen, Liu, & Xu, 2014). Therefore, inexpensive, and more practical quantitative measurement methods, yet selective, need to be developed. One of them is the metal nanoparticles-based colorimetric sensor. The colorimetric method is easier and more practical because the measurement result can be observed visually based on a color change. In addition, colorimetric sensors allow real-time qualitative and quantitative analyses (Chen, Han, Yang, & Pu, 2017; Firdaus et al., 2017; Taufiq, Eden, Sumarni, & Alauhdin, 2021).

The principle of metal nanoparticles-based colorimetry is the Localized Surface Plasmon Resonance (LSPR) phenomenon of metal nanoparticles. LSPR is a specific property of metal

nanoparticles related to the collective oscillation of conduction electrons when interacting with visible light. Thus, a nanoparticle suspension will exhibit a characteristic color. An external disturbance may change the color due to interparticle plasmon incorporation which then inducing a shift in the LSPR absorption band (Zhang, & Noguez, 2008). This can be applied as the basis of colorimetric analysis.

One of the metal nanoparticles that is widely applied in colorimetric sensors is silver nanoparticles (AgNPs). Several AgNPs-based colorimetric assays have been developed for the detection of metal ions, such as Hg(II) (Firdaus et al., 2017), Cu(II) (Taufiq et al., 2021), Pb(II) (Shrivastava et al., 2019), Mn(II) (He, & Zhang, 2016), and Zn(II) ions (Lee et al., 2016). In addition, AgNPs have also been applied to the colorimetric sensing of hydrogen peroxide (Rizqi & Alauhdin, 2021; H. Wang et al., 2017). Several parameters need to be achieved by an analytical sensor, one of them is selectivity. A selective metal ion sensor can avoid interference by other metal ions. The use of AgNPs for Hg(II) detection has been carried out (Bothra, Solanki, & Sahoo, 2013; Firdaus et al., 2017), but the effect of interfering metal ions need to be investigate further.

Silver nanoparticles can be synthesized by chemical reduction. This method is simple, easy, and effective to produce AgNPs. In this method, a reducing agent is

needed to reduce Ag(I) to Ag(0) which then forms nanocolloidal AgNPs. AgNPs as a nanocolloid are usually stabilized by a stabilizing agent (Pimpang, Sutham, Mangkorntong, Mangkorntong, & Choopun, 2008). Controlling the size and shape of nanoparticles during synthesis is crucial since they have an impact on the properties of nanoparticles, particularly the LSPR absorption spectrum. Several biopolymers were used as the stabilizing agent which can control the formation of nanoparticles and stabilize metal dispersions. Some of these biopolymer reagents include lignin (Aadil, Pandey, Mussatto, & Jha, 2019), chitosan (Junaidi, Wahyudi, & Umaningrum, 2015; Twu, Chen, & Shih, 2008), and cellulose (Ogundare, & van Zyl, 2018). The free polymer chains provide a steric hindrance effect on the AgNPs, so that aggregation can be avoided (Huang et al., 1996; Luo et al., 2005).

Chitosan is a linear polysaccharide resulting from the deacetylation of chitin. The reactivity of chitosan is influenced by amine ($-NH_2$) and hydroxyl ($-OH$) groups in each monomer. These groups can interact with transition metal cations to form chitosan-metal complexes (Wang, Du, Fan, Liu, & Hu, 2005). Earlier researchers have studied the use of chitosan as a stabilizing agent in AgNPs synthesis (Alexandrova, Futoryanskaya, & Sadykova, 2020; Junaidi et al., 2015; Twu et al., 2008). This stabilizing agent is critical for the formation of uniformly sized and well-dispersed nanoparticles.

In this study, AgNPs-chitosan (AgNPs-Ch) was synthesized by chemical reduction using silver nitrate as a precursor. Meanwhile, biopolymer chitosan and trisodium citrate were used as stabilizer and reducing agents, respectively. The synthesized AgNPs-Ch was tested for its application as a metal ion sensor of Hg(II). The linearity, sensitivity, and selectivity of AgNPs-Ch for mercury(II) ions were determined to evaluate its performance. Interfering ions were added into Hg(II) sample solution to examine the selectivity of AgNPs-Ch as a sensor probe.

EXPERIMENTAL SECTION

Materials

Silver nitrate ($AgNO_3$) as a precursor of AgNPs, reductor trisodium citrate ($Na_3C_6H_5O_7$), and acetic acid ($HC_2H_3O_2$, 96%) were supplied by Merck. Salt of cations for sensor performance testing were also supplied by Merck. Meanwhile, chitosan (75-85% deacetylated) was purchased from Sigma Aldrich and used without further purification.

Synthesis of AgNPs-Ch

AgNPs-Ch synthesis was carried out by reacting $AgNO_3$ 1mM, chitosan 1% (prepared in acetic acid 1%) and sodium citrate 1%. The reaction mixture was then heated at various temperature i.e., 27°C, 60°C, 80°C, and 100°C with stirring for 60 minutes.

The obtained colloidal AgNPs-Chs were initially characterized by a UV-Visible Spectrophotometer

(Flourence BMG Labtech). The formation of silver nanoparticle was detected by scanning absorption spectra in the range of 200–600 nm.

For Transmission Electron Microscopy (TEM) imaging, the colloidal AgNPs-Ch sample was dropped onto carbon coated grids and then allowed to dry at ambient temperature. The imaging was completed using a JEOL JEM-1400 operating at an accelerating voltage of 120 kV. Particle size was obtained from the TEM images and calculated using ImageJ software from 60 particles.

Detection of metal ions

To examine the sensing property of synthesized AgNPs-Ch, various transition metal ions including Pb(II), Cd(II), Zn(II), and Hg(II) were used at a concentration of 500 ppm. The metal ion solutions were added into the colloidal AgNPs-Ch drop wise in the ratio of 1:2. The spectra of the mixture were observed using a UV-Visible Spectrophotometer at wavelength of 200 - 800 nm. The AgNPs-Ch response for metal ions was presented as Δ absorbance (ΔA), calculated using the following equation:

$$\Delta A = A_{(AgNPs-Ch)} - A_{(AgNPs-Ch+metal\ ion)}$$

where $A_{(AgNPs-Ch)}$: absorbance of AgNPs-Ch in the absence of metal ion, $A_{(AgNPs-Ch+metal\ ion)}$: absorbance of AgNPs-Ch in the presence of metal ion(s).

Performance of AgNPs-Ch on Hg(II) detection

The sensing performance of AgNPs-Ch was observed further on the Hg(II) detection. It included linearity, sensitivity, and selectivity. Linearity was measured in Hg(II) concentration range of 1 – 5 ppm. Sensitivity was measured as LoD and LoQ values from standard deviation (σ) of the slope of linearity plot. LoD is $3.3\sigma/\text{slope}$, while LoQ is $10\sigma/\text{slope}$.

The selectivity of AgNPs-Ch toward Hg(II) was examined using interfering metal ions, such as Fe(III), Cd(II), Zn(II), and Pb(II). The concentration of Hg(II) and the interfering ions were all 10 ppm. Measurement was carried out by mixing AgNPs-Ch with Hg(II) in the absence and presence of interfering ions. The UV-vis spectra were then recorded at wavelength of 200 - 600 nm.

RESULTS AND DISCUSSION

Characteristics of AgNPs-Ch

AgNPs were resulted by the reduction of Ag(I) using trisodium citrate. Initially, Ag(I) formed Ag(I)/Chitosan complex (Twu et al., 2008) which then allowed the Ag(I) to collect electrons from citrate and be reduced to an Ag atom. Here, chitosan could also participate in the reduction reaction. However, its reducing energy is low (Susilowati et al., 2019), as a result, the main reducing agent in the reaction was trisodium citrate. Meanwhile, chitosan polymers through their amine ($-NH_2$) and hydroxyl ($-OH$) groups covering and stabilizing the formed nanoparticles (Figure 1).

The formation of AgNPs is indicated by the appearance of a yellowish-brown color due to the LSPR absorption of AgNPs when exposed to visible light (Hammond, Bhalla, Rafiee, & Estrela, 2014). The LSPR absorption was monitored by a UV-vis spectrophotometer and shown in **Figure 2**. The formation of AgNPs with chitosan as a reducing agent resulted in an absorbance of 0.348 at a wavelength of 414 nm, while the addition of trisodium citrate resulted in a higher absorbance of 0.955 at a wavelength of 427 nm (**Figure 2a**). This presented that chitosan can act as a reducing agent but is not quite strong to reduce Ag(I) to Ag(0). Previous report showed that chitosan can be used to reduce silver ions, but it requires 12 hours of reaction at 95°C (Wei et al., 2009).

At initial reaction, 30 and 60 minutes (**Figure 2b**), the absorption peaks were low and broad, these indicated low concentration of AgNPs formed with broad size distribution. After 240 minutes, the peak was getting higher and narrower. It means there were more AgNPs formed with more uniform size. Meanwhile, measurement of LSPR absorption at 4th and 7th day showed constant absorption peaks at the same wavelength as initial. Thus, the AgNPs-Ch were stable until the 7th day of synthesis. This stable condition could be obtained in the presence of chitosan. Free polymer chains of chitosan provide steric hindrance which prevent the AgNPs aggregation. This stabilization mechanism was also obtained on the use of Polyethylene Glycol (PEG) in the

AgNPs synthesis (Luo, Zhang, Zeng, Zeng, & Wang, 2005).

Figure 3 shows that AgNPs-Ch synthesis is affected by temperature. Based on the visible spectra, silver nanoparticles begin to form at a temperature of 80°C. This is indicated by the appearance of intense absorption peak at 427 nm and the appearance of yellowish-brown which is the typical color of nanocolloidal AgNPs. In addition, the transparent appearance indicating good dispersity of the particles in water. Likewise at a temperature of 100°C, the LSPR band appears at a wavelength of 430 nm with pale-yellow color. However, the absorption peak was lower than that of AgNPs-Ch at 80°C. According to Luo, the reaction temperature plays an important role in the dimensions of AgNPs, where the particles size enlarged when the temperature was raised (Luo et al., 2005). The reduction of Ag(I) resulted silver metal, Ag(0), that will undergo a nucleation phase to form silver nanoparticles (AgNPs) and provide a typical absorption peak around 400 nm as a result of the LSPR phenomenon. The formed AgNPs was then stabilized by chitosan polymers. The stabilator is an important agent in the synthesis of colloidal AgNPs. The presence of a single absorption of Visible spectra around 400 nm implies that the synthesized nanoparticles are spherical (Guzmán, Dille, & Godet, 2009). The spherical particles can also be seen from the TEM image (**Figure 4**). Based on the TEM images, the nanoparticles had an average particle size of 14.33 ± 4.20 nm.

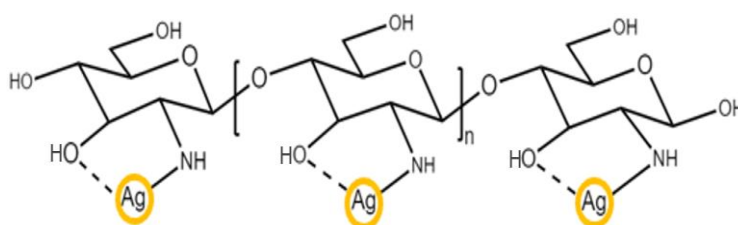


Figure 1. The amine ($-\text{NH}_2$) and hydroxyl ($-\text{OH}$) of chitosan covering and stabilizing AgNPs

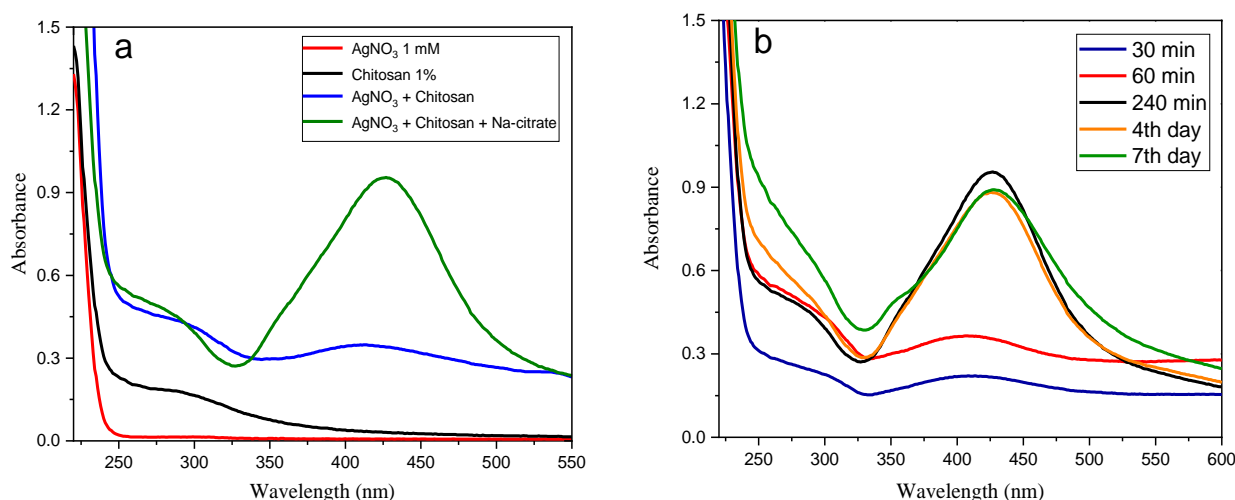


Figure 2. a) The UV-visible spectra of a) AgNPs-Ch prepared with and without $\text{Na}_3\text{-citrate}$, b) The growth and stability of AgNPs-Ch

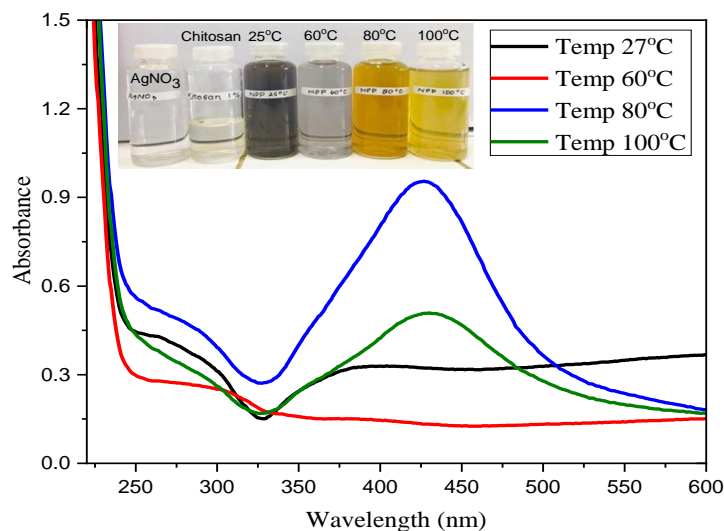


Figure 3. The UV-visible spectra of nanocolloidal AgNPs-Ch prepared at different temperature. Insert: a digital image showing the color of resulted colloids at different synthesis temperature.

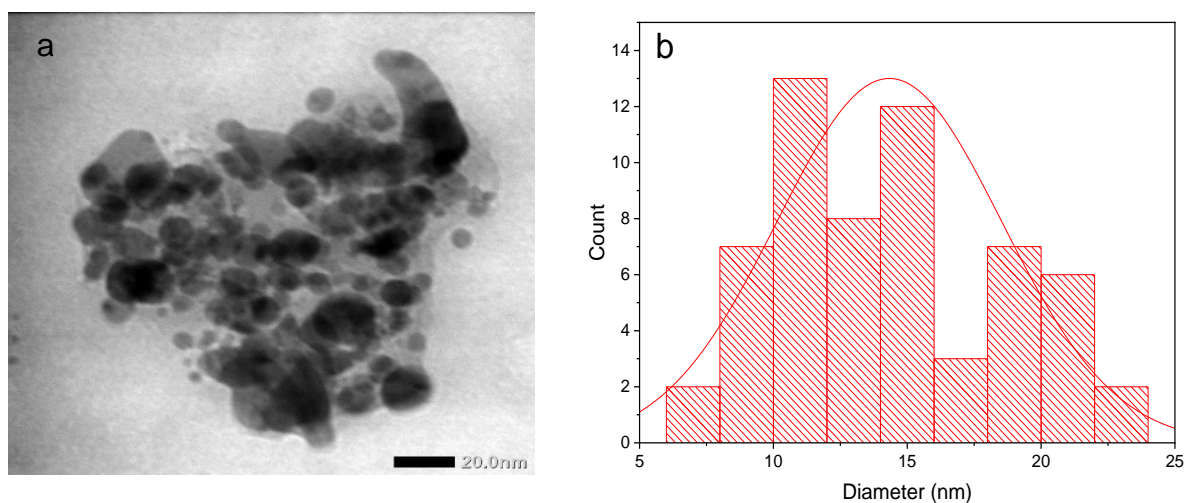


Figure 4. a) TEM image of AgNPs-Ch produced at 80°C. Scale bar: 20 nm, b) particle size distribution

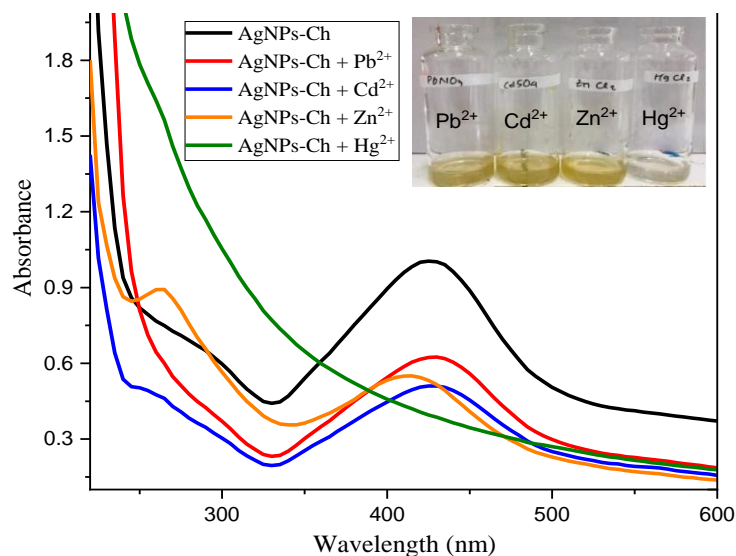


Figure 5. The UV-Vis spectra of AgNPs-Ch in the presence of 500 ppm Pb(II), Cd(II), Zn(II) and Hg(II). Insert: a digital image showing the color of AgNPs-Ch after addition of the metal ions.

Detection of Hg(II)

The AgNPs-Ch produced at 80°C was tested as a colorimetric probe of Hg(II) metal ions. Initially, several metal ions namely Pb(II), Cd(II), Zn(II) and Hg(II) were tested to observe the response of AgNPs-Ch to these metal ions (**Figure 5**). This preliminary study showed that AgNPs-Ch was more sensitive to Hg(II) than the other three metal ions tested. In the presence of mercury ion, Hg(II), the color of colloidal AgNPs-Ch changed from yellowish-brown to a clear and transparent suspension. Moreover, the presence of Hg(II) leads to a significant decrease of the absorption of AgNPs-Ch, providing a positive indicator for sensitive detection. Meanwhile, the addition of Pb(II), Cd(II) and Zn(II) ions did not change the color of the colloid visually. This is in accordance with the results of the visible spectra (**Figure 5**) which showed a decrease in absorbance without shifting the peaks significantly of those ions addition. These results showed that the AgNPs-Ch are favorable to sensitive and selective detection of Hg(II).

The proposed detection mechanism that may apply is due to Hg(II) induced-deprotection followed by spontaneous oxidation of Ag(0). The introduction of

Hg(II) into AgNPs-Ch colloid interfered the interaction of AgNPs and chitosan. This causes the AgNPs to destabilize. Then, the destabilized-AgNPs will be oxidized spontaneously by Hg(II) as it has a higher reduction potential ($E_{\text{Hg}^{2+}/\text{Hg}_2^{2+}}^0: +0.908 \text{ V}$ or $E_{\text{Hg}^{2+}/\text{Hg}}^0: +0.852 \text{ V}$) than Ag(I) ($E_{\text{Ag}^+/\text{Ag}}^0: +0.799 \text{ V}$). The oxidation of AgNPs or Ag atomic to Ag(I) causes disappearing of LSPR absorption and yellow color in AgNPs-Ch colloids. The higher the Hg(II) concentration, the faster and clearer the yellow color disappears. The destabilized AgNPs may also aggregated as the distance between particles become closer, then resulting a bigger particles and shifting the LSPR band to a longer wavelength (Firdaus et al., 2017; Lee et al., 2016). In fact, the destabilization of AgNPs may also occur in the presence of other metal ions; (Pb(II), Cd(II) and Zn(II)). However, the other metal ions have a lower reduction potential than Ag(I). Thus, the spontaneous reaction between Ag(I) and Pb(II), Cd(II), or Zn(II) did not occur. As a result, there is no LSPR shifting or color changing when those ions added into the AgNPs-Ch colloids. This proposed sensing mechanism is presented in **Figure 6**.

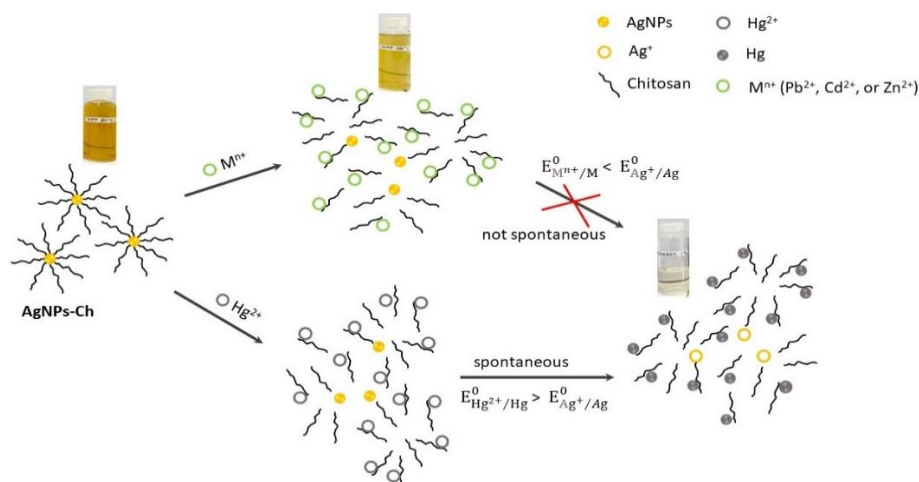


Figure 6. The proposed detection mechanism of Hg^{2+} by AgNPs-Ch nanocolloid

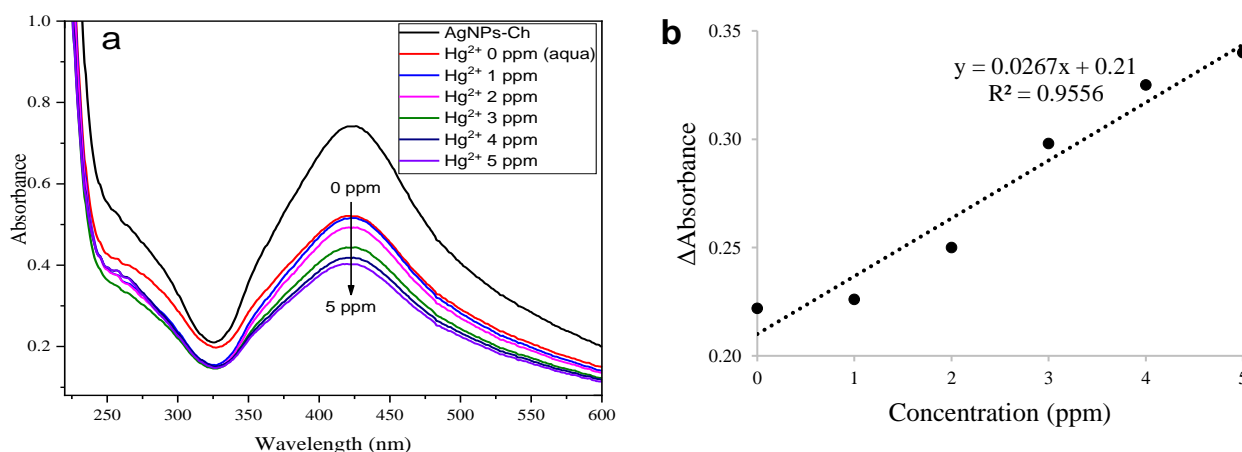


Figure 7. a) The UV-Vis spectra of AgNPs-Ch in the presence of Hg(II) at different concentration, b) linearity curve of the Hg(II) detection.

Furthermore, the performance of AgNPs-Ch in detecting Hg(II) ions was tested for validity which included linearity, sensitivity, and selectivity. The linearity for the detection of Hg(II) ions was determined by visible spectrophotometry in the concentration range between 1 ppm and 5 ppm. The higher the mercury(II) concentration, the smaller the absorbance of AgNPs-Ch and the color intensity was getting lower (**Figure 7a**).

Based on the visible spectra, the increase of Hg(II) concentration resulted on the decreasing LSPR band of AgNPs-Ch with a coefficient of determination (r^2) of 0.9556 (**Figure 7b**). This showed that there is a linear dependent between the absorbance of AgNPs-Ch and the concentration of Hg(II) ions, especially in the concentration range of 1 - 5 ppm. Meanwhile, the detection limit of AgNPs-Ch for Hg(II) ions was 1.33 ppm, while the limit of quantization was 4.03 ppm. It means that the lowest concentration of Hg(II) that could be detected by AgNPs was 1.33 ppm, while the lowest concentration of Hg(II) that could be determined precisely for quantitative analysis was 4.03 ppm. When compared to the colorimetric detection of Hg(II) utilizing other AgNPs-based probes, this result was highly encouraging (**Table 1**). However, the proposed method has not been able to compete

with established analytical methods such as Cold vapor-atomic absorption spectroscopy (CV-AAS) and the more advanced instrument, Capillary electrophoresis-inductively coupled plasma mass spectrometry (CE-ICP-MS). Furthermore, the detection limit of this method remains higher than that of AuNPs-based colorimetric methods.

In addition, the sensitivity and selectivity could be increased further, for example by adding a specific capping agent on the surface of AgNPs or by applying preconcentration step as an initial procedure. The preconcentration step can also be used to eliminate a complicated matrix from the samples that could interfere the analysis process. Furthermore, the suggested AgNPs approach has advantages. It is not only simple and inexpensive but also has the benefit of being able to be adjusted for field applications using digital image colorimetry (Ratnarathorn et al., 2012; Shrivastava et al., 2019).

Moreover, the selectivity of the Hg(II) detection was tested in the presence of interfering metal ions in a solution. The solution contained Hg(II) ions and one or two interfering ions, such as Pb(II), Fe(III), Cd(II) and Zn(II) with a concentration of 10 ppm. The results of this selectivity test can be seen in **Figure 8** and **Figure 9**.

Table 1. The limit of detection (LoD) for Hg(II) analysis of the proposed method compare to previously reported methods.

Method	Probe	LoD (ppm)	Reference
CE-ICP-MS	-	0.000027	(Zhao et al., 2012)
CV-AAS	-	0.002	(Coelho-Souza et al., 2011)
Colorimetry	poly(acrylamide-co-methylenbisacrylamide) nanocomposite	0.001	(Sedghi et al., 2015)
Colorimetry	hexadecyltrimethylammonium bromide (CTAB)-coated AuNPs	0.024	(Jin & Han, 2014)
Colorimetry	NaCysC stabilized-AgNPs	0.0016	(Annadhasan & Rajendiran, 2015)
Colorimetry	Flavonoid capped-AgNPs	17.05	(Firdaus et al., 2017)
Colorimetry	AgNPs-chitosan	1.33	This work

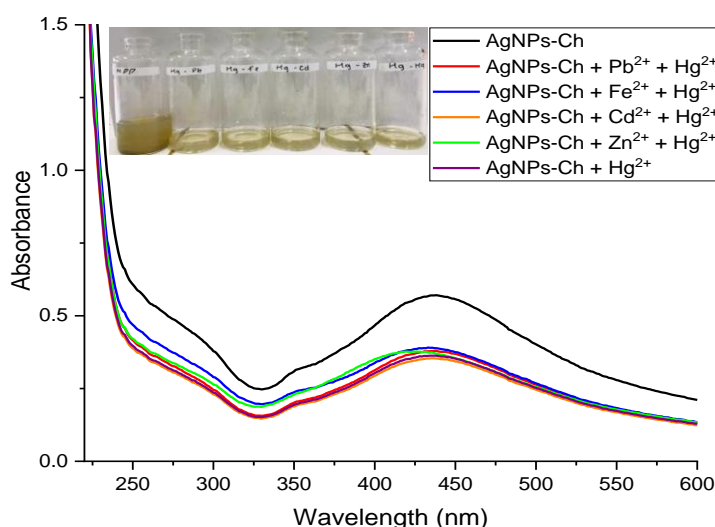


Figure 8. The UV-Vis spectra of the selectivity test of AgNPs-Ch towards Hg(II) in the presence of an interfering metal ion. The concentration of all ions is 10 ppm.

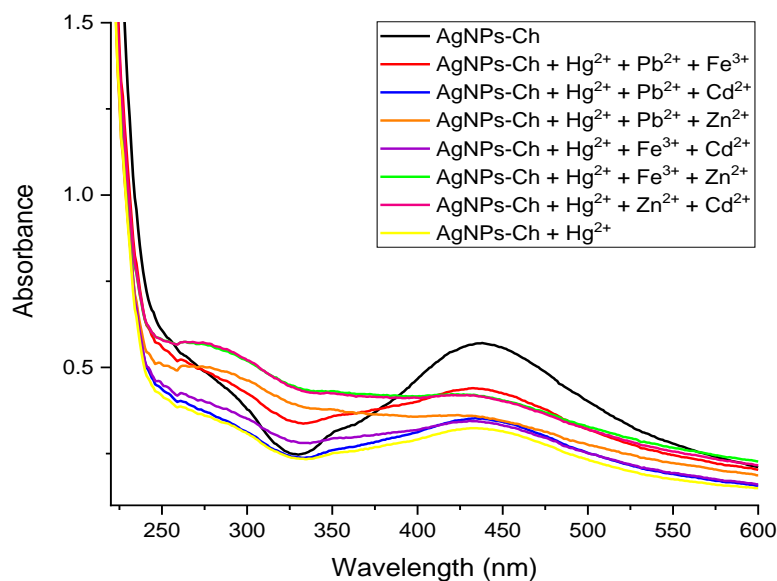


Figure 9. The UV-Vis spectra of the selectivity test of AgNPs-Ch towards Hg(II) in the presence of two interfering metal ions. The concentration of all ions is 10 ppm.

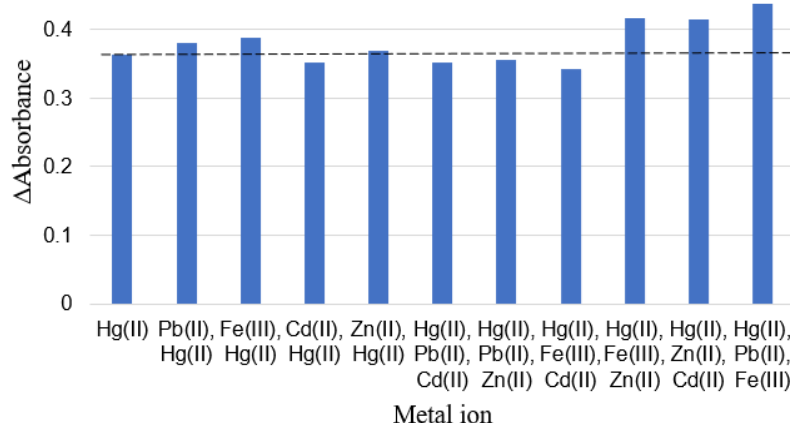


Figure 10. The Δ absorbance of AgNPs-Ch in the presence of Hg(II) and interfering metal ions

Visually, the presence of interfering ions had no effect on the coloration of the AgNPs-Ch. Thus, it can be concluded that the color change was only affected by the interaction of AgNPs-Ch with Hg(II) ions. This was supported by visible spectra data where the absorbance peak of [NPP-chitosan + Hg(II)] was not significantly different from the peak of [NPP-chitosan + Hg(II) + an interfering ion], which was less than 3.0% (**Figure 10**). Meanwhile, in the case of addition of two interfering ions, the highest Δ absorbance occurred in the combination of Hg(II), Pb(II), and Fe(III), which was 7.5%.

According to the results, the presence of Fe(III) as a single ion or combined with other ions contributed to the largest interference on the AgNPs-Ch response to Hg(II). It was known that Fe(III) has the highest reduction potential standard among the other interfering ions tested. This Fe(III) effect has also been occurred previously on the detection of Hg(II) using AgNPs functionalized by *p*-phenylenediamine (*p*-PDA) (Bothra et al., 2013).

CONCLUSIONS

Silver nanoparticles-chitosan (AgNPs-Ch) can be synthesized by chemical reduction method at 80°C using silver nitrate and sodium citrate as precursor and reducing agent, respectively. The synthesized nanoparticles were spherical with an average size of 14.33 ± 4.20 nm. Testing for metal ion detection showed that AgNPs-Ch was selective for mercury metal ion, Hg(II) with a linearity of 0.9556 in the concentration range of 1 - 5 ppm and was able to detect the ion down to 1.33 ppm.

ACKNOWLEDGMENTS

The authors thank Dr. Sri Kadarwati for the valuable suggestion and input on this article.

REFERENCES

- Aadil, K. R., Pandey, N., Mussatto, S. I., & Jha, H. (2019). Green synthesis of silver nanoparticles using acacia lignin, their cytotoxicity, catalytic, metal ion sensing capability and antibacterial

- activity. *Journal of Environmental Chemical Engineering*, 7(5), 103296. <https://doi.org/10.1016/j.jece.2019.103296>
- Alexandrova, V. A., Futoryanskaya, A. M., & Sadykova, V. S. (2020). Silver Nanoparticles Stabilized with Chitosan Succinamide: Synthesis and Antibacterial Activity. *Applied Biochemistry and Microbiology*, 56(5), 590–594. <https://doi.org/10.1134/S0003683820050026>
- Annadhasan, M., & Rajendiran, N. (2015). Highly selective and sensitive colorimetric detection of Hg(II) ions using green synthesized silver nanoparticles. *RSC Adv.*, 5(115), 94513–94518. <https://doi.org/10.1039/C5RA18106B>
- Bothra, S., Solanki, J. N., & Sahoo, S. K. (2013). Functionalized silver nanoparticles as chemosensor for pH, Hg²⁺ and Fe³⁺ in aqueous medium. *Sensors and Actuators B: Chemical*, 188, 937–943. <https://doi.org/https://doi.org/10.1016/j.snb.2013.07.111>
- Chen, Y., Han, S., Yang, S., & Pu, Q. (2017). Rhodanine stabilized gold nanoparticles for sensitive and selective detection of mercury (II). *Dyes and Pigments*, 142, 126–131. <https://doi.org/10.1016/j.dyepig.2017.03.022>
- Cheng, H., Wu, C., Shen, L., Liu, J., & Xu, Z. (2014). Online anion exchange column preconcentration and high performance liquid chromatographic separation with inductively coupled plasma mass spectrometry detection for mercury speciation analysis. *Analytica Chimica Acta*, 828, 9–16. <https://doi.org/10.1016/j.aca.2014.04.042>
- Coelho-Souza, S. A., Guimarães, J. R. D., Miranda, M. R., Poirier, H., Mauro, J. B. N., Lucotte, M., & Mergler, D. (2011). Mercury and flooding cycles in the Tapajós river basin, Brazilian Amazon: The role of periphyton of a floating macrophyte (*Paspalum repens*). *Science of The Total Environment*, 409(14), 2746–2753. <https://doi.org/https://doi.org/10.1016/j.scitotenv.2011.03.028>
- Fernández, Z. H., Valcárcel Rojas, L. A., Álvarez, A. M., Estevez Álvarez, J. R., Araújo dos Santos, J., González, I. P., González, M. R., Macías, N. A., Sánchez, D. L., & Torres, D. H. (2015). Application of Cold Vapor-Atomic Absorption (CVAAS) Spectrophotometry and Inductively Coupled Plasma-Atomic Emission Spectrometry methods for cadmium, mercury and lead analyses of fish samples. Validation of the method of CVAAS. *Food Control*, 48, 37–42. <https://doi.org/10.1016/j.foodcont.2014.05.056>
- Firdaus, M. L., Fitriani, I., Wyantuti, S., Hartati, Y. W., Khaydarov, R., McAlister, J. A., Obata, H., & Gamo, T. (2017). Colorimetric Detection of Mercury(II) Ion in Aqueous Solution Using Silver Nanoparticles. *Analytical Sciences*, 33(7), 831–837. <https://doi.org/10.2116/analsci.33.831>
- Guzmán, M. G., Dille, J., & Godet, S. (2009). Synthesis of silver nanoparticles by chemical reduction method and their antibacterial activity. *Int. J. Chem. Biol. Eng.*, 2, 104–111.
- Hammond, J. L., Bhalla, N., Rafiee, S. D., & Estrela, P. (2014). Localized Surface Plasmon Resonance as a Biosensing Platform for Developing Countries. In *Biosensors* (Vol. 4, Issue 2). <https://doi.org/10.3390/bios4020172>
- He, Y., & Zhang, X. (2016). Ultrasensitive colorimetric detection of manganese(II) ions based on anti-aggregation of unmodified silver nanoparticles. *Sensors and Actuators, B: Chemical*, 222, 320–324. <https://doi.org/10.1016/j.snb.2015.08.089>
- Huang, H. H., Ni, X. P., Loy, G. L., Chew, C. H., Tan, K. L., Loh, F. C., Deng, J. F., & Xu, G. Q. (1996). Photochemical Formation of Silver Nanoparticles in Poly(N-vinylpyrrolidone). *Langmuir*, 12(4), 909–912. <https://doi.org/10.1021/la950435d>
- Jin, L.-H., & Han, C.-S. (2014). Eco-friendly colorimetric detection of mercury(II) ions using label-free anisotropic nanogolds in ascorbic acid solution. *Sensors and Actuators B: Chemical*, 195, 239–245. <https://doi.org/https://doi.org/10.1016/j.snb.2014.01.020>
- Junaidi, A. B., Wahyudi, A., & Umaningrum, D. (2015). Sintesis AgNPs Secara Reduksi Kimia Menggunakan Capping Agent Kitosan dan Pereduksi Glukosa. *Sains Dan Terapan Kimia*, 9(2), 70–80.
- Kristian, K. E., Friedbauer, S., Kabashi, D., Ferencz, K. M., Barajas, J. C., & O'Brien, K. (2015). A Simplified Digestion Protocol for the Analysis of Hg in Fish by Cold Vapor Atomic Absorption Spectroscopy. *Journal of Chemical Education*, 92(4), 698–702. <https://doi.org/10.1021/ed500687b>
- Lee, S., Nam, Y. S., Lee, H. J., Lee, Y., & Lee, K. B. (2016). Highly selective colorimetric detection of Zn(II) ions using label-free silver nanoparticles. *Sensors and Actuators, B: Chemical*, 237, 643–651. <https://doi.org/10.1016/j.snb.2016.06.141>
- Luo, C., Zhang, Y., Zeng, X., Zeng, Y., & Wang, Y. (2005). The role of poly(ethylene glycol) in the formation of silver nanoparticles. *Journal of Colloid and Interface Science*, 288(2), 444–448. <https://doi.org/https://doi.org/10.1016/j.jcis.2005.03.005>
- Ogundare, S. A., & van Zyl, W. E. (2018). Nanocrystalline cellulose as reducing- and stabilizing agent in the synthesis of silver nanoparticles: Application as a surface-enhanced Raman scattering (SERS) substrate. *Surfaces and Interfaces*, 13, 1–10.

- <https://doi.org/10.1016/j.surfin.2018.06.004>
- Pimpang, P., Sutham, W., Mangkorntong, N., Mangkorntong, P., & Choopun, S. (2008). Effect of stabilizer on preparation of silver and gold nanoparticle using grinding method. *Chiang Mai J Sci*, 35(1), 250–257.
- Ratnarathorn, N., Chailapakul, O., Henry, C. S., & Dungchai, W. (2012). Simple silver nanoparticle colorimetric sensing for copper by paper-based devices. *Talanta*, 99, 552–557. <https://doi.org/https://doi.org/10.1016/j.talanta.2012.06.033>
- Rizqi, P., & Alauhdin, M. (2021). Silver nanoparticles synthesis with kersen leaf extract (*Muntingia calabura* L.) as areductor and its application for hydrogen peroxide detection. *IJCS*, 10(1), 27–34.
- Sedghi, R., Heidari, B., & Behbahani, M. (2015). Synthesis, characterization and application of poly(acrylamide-co-methylenbisacrylamide) nanocomposite as a colorimetric chemosensor for visual detection of trace levels of Hg and Pb ions. *Journal of Hazardous Materials*, 285, 109–116. <https://doi.org/https://doi.org/10.1016/j.jhazmat.2014.11.049>
- Shrivas, K., Sahu, B., Deb, M. K., Thakur, S. S., Sahu, S., Kurrey, R., Kant, T., Patle, T. K., & Jangde, R. (2019). Colorimetric and paper-based detection of lead using PVA capped silver nanoparticles: Experimental and theoretical approach. *Microchemical Journal*, 150, 104156. <https://doi.org/10.1016/J.MICROC.2019.104156>
- Susilowati, E., Maryani, & Ashadi. (2019). Green synthesis of silver-chitosan nanocomposite and their application as antibacterial material. *Journal of Physics Conf. Series*, 1153, 1–7.
- Taufiq, M., Eden, W. T., Sumarni, W., & Alauhdin, M. (2021). Colorimetric detection of metal ions using green-synthesized silver nanoparticles. *Journal of Physics: Conference Series*, 1918, 1–6.
- Twu, Y. K., Chen, Y. W., & Shih, C. M. (2008). Preparation of silver nanoparticles using chitosan suspensions. *Powder Technology*, 185(3), 251–257. <https://doi.org/10.1016/j.powtec.2007.10.025>
- Wang, H., Wang, H., Li, T., Ma, J., Li, K., & Zuo, X. (2017). Silver nanoparticles selectively deposited on graphene-colloidal carbon sphere composites and their application for hydrogen peroxide sensing. *Sensors and Actuators, B: Chemical*, 239, 1205–1212. <https://doi.org/10.1016/j.snb.2016.08.143>
- Wang, X., Du, Y., Fan, L., Liu, H., & Hu, Y. (2005). Chitosan- metal complexes as antimicrobial agent: Synthesis, characterization and Structure-activity study. *Polymer Bulletin*, 55(1), 105–113. <https://doi.org/10.1007/s00289-005-0414-1>
- Wei, D., Sun, W., Qian, W., Ye, Y., & Ma, X. (2009). The synthesis of chitosan-based silver nanoparticles and their antibacterial activity. *Carbohydrate Research*, 344(17), 2375–2382. <https://doi.org/10.1016/j.carres.2009.09.001>
- Zhang, J. Z., & Noguez, C. (2008). Plasmonic Optical Properties and Applications of Metal Nanostructures. *Plasmonics*, 3(4), 127–150. <https://doi.org/10.1007/s11468-008-9066-y>
- Zhao, Y., Zheng, J., Fang, L., Lin, Q., Wu, Y., Xue, Z., & Fu, F. (2012). Speciation analysis of mercury in natural water and fish samples by using capillary electrophoresis-inductively coupled plasma mass spectrometry. *Talanta*, 89, 280–285. <https://doi.org/10.1016/j.talanta.2011.12.029>
- Zierhut, A., Leopold, K., Harwardt, L., & Schuster, M. (2010). Analysis of total dissolved mercury in waters after on-line preconcentration on an active gold column. *Talanta*, 81(4–5), 1529–1535. <https://doi.org/10.1016/j.talanta.2010.02.064>